

● *Original Contribution***QUANTIFICATION OF MICROBUBBLE DESTRUCTION OF THREE FLUOROCARBON-FILLED ULTRASONIC CONTRAST AGENTS**

CARMEL M. MORAN, T. ANDERSON, S. D. PYE, V. SBOROS and W. N. McDICKEN

Department of Medical Physics and Medical Engineering, University of Edinburgh, Edinburgh, Scotland, UK

(Received 31 August 1999; in final form 12 January 2000)

Abstract—The assessment of myocardial blood velocity using ultrasonic contrast agents is based on the premise that the vast majority of contrast microbubbles within a myocardial region can be destroyed by an acoustic pulse of sufficient magnitude. Determination of the period of time after destruction that a region of myocardium needs to reperfuse may be used to assess myocardial blood velocity. In this study, we investigated the acoustic pressure sensitivity of three solutions of intravenous fluorocarbon-filled contrast agents and the magnitude of acoustic pulse required to destroy the contrast agent microbubbles. A novel tissue-mimicking phantom was designed and manufactured to investigate the relationships between mean integrated backscatter, incident acoustic pressure and number of frames of insonation for three fluorocarbon-filled contrast agents (Definity®, Optison®, and Sonazoid®, formerly NC100100). Using a routine clinical ultrasound (US) scanner (Acuson XP-10), modified to allow access to the unprocessed US data, the contrast agents were scanned at the four acoustic output powers. All three agents initially demonstrated a linear relationship between mean integrated backscatter and number of frames of insonation. For all three agents, mean integrated backscatter decreased more rapidly at higher acoustic pressures, suggesting a more rapid destruction of the microbubbles. In spite of the fact that there was no movement of microbubbles into or out of the beam, only the results from Definity® suggested that a complete destruction of the contrast agent microbubbles had occurred within the total duration of insonation in this study. © 2000 World Federation for Ultrasound in Medicine & Biology.

Key Words: Ultrasound, Ultrasonic contrast agents, DMP115, Definity®, Sonazoid®, NC100100, Optison®, Tissue-mimicking phantom, Echocardiography.

INTRODUCTION

Optimising the performance of ultrasonic contrast agents *in vivo* requires an in-depth knowledge of the interaction of the contrast agent microbubbles and the incident acoustic pressure wave. Parameters such as the stiffness and elasticity of the microbubble shell and the type of encapsulated gas significantly affect the acoustical behaviour of the microbubble (Dayton et al. 1999; Strauss and Beller 1999). It has previously been shown that the magnitude of the acoustic pressure pulse emitted from routine clinical scanners has sufficient energy to cause the microbubbles to behave in a nonlinear manner (Schrope et al. 1992). Such nonlinear behaviour has been exploited in new imaging modalities such as second harmonic imaging (Schrope et al. 1992; Chang et al. 1995) and pulse inversion imaging (Simpson et al. 1999).

Both techniques display images formed predominantly from the nonlinear portions of the backscattered ultrasound (US) signal. Furthermore, it has been shown that contrast microbubbles, when insonated with acoustic pressures of sufficient magnitude, can rupture, releasing free gas bubbles (Porter and Xie 1995; Porter et al. 1997) that scatter US much more effectively than their encapsulated counterparts (Church 1995). Because the lifetime of such bubbles is on the order of milliseconds, such scattering is short-lived. Consequently, US imaging techniques intended to exploit this phenomenon use high acoustic output pressures and a variable triggered imaging mode to allow sufficient time for reperfusion between consecutive scanning frames. One such application of the technique currently being explored is the detection of myocardial perfusion defects (Marwick et al. 1998; DeMaria and Cotter 1998). It has been suggested that the time period between destruction of contrast microbubbles and subsequent contrast re-enhancement of the myocardium is related to mean myocardial blood velocity (Wei et al. 1998; Linka et al. 1998; Pelberg et al.

Address correspondence to: Carmel M. Moran, Department of Medical Physics and Medical Engineering, University of Edinburgh, 1 Lauriston Place, Edinburgh EH3 9YW Scotland, UK. E-mail: carmel.moran@ed.ac.uk

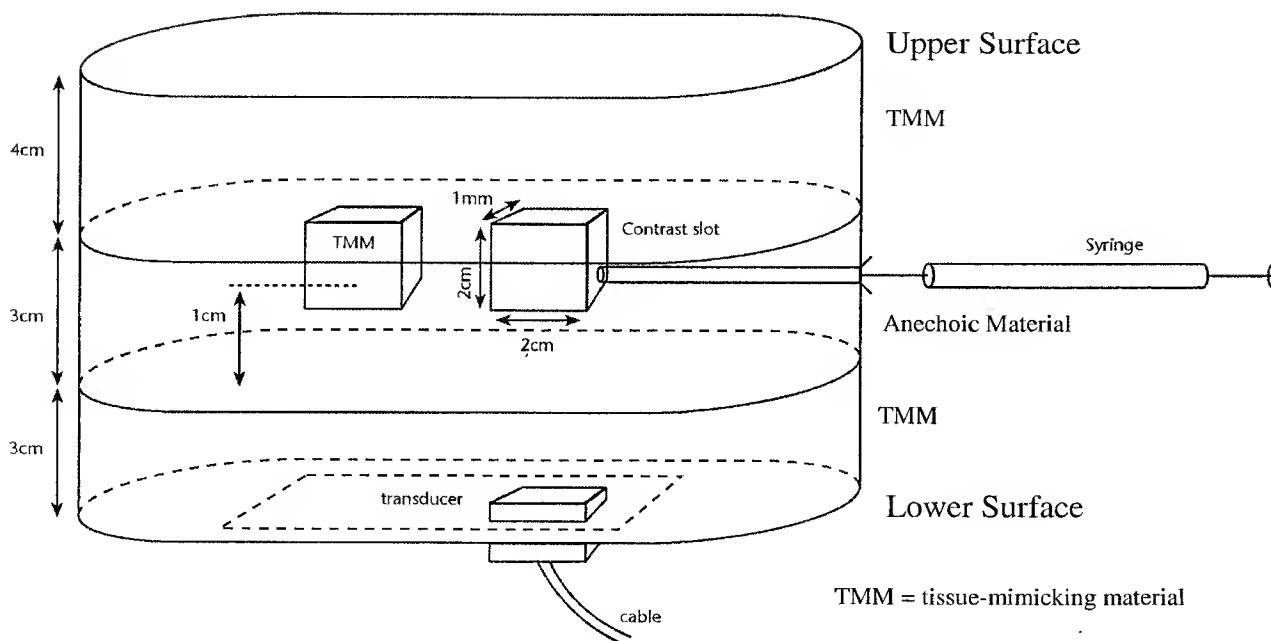


Fig. 1. Schematic diagram of phantom.

1999). An assumption underlying this technique is that, effectively, all contrast microbubbles within a myocardial region can be destroyed by a sufficiently large diagnostic pulse. However, although it is accepted that the thresholds at which the destruction phenomenon takes place are dependent on the microbubble shell characteristics, the actual magnitude of this threshold has not been adequately investigated for contrast agents either being routinely used or currently undergoing clinical trials. Previous work, with a limited range of contrast agents, has shown that these thresholds do exist (Frinking et al. 1999; Moran et al. 1998; Wei et al. 1997). The aim of this study was to establish the acoustic pressure sensitivity of three fluorocarbon-filled contrast agents and to attempt to quantify how their backscatter varies as a function of insonation time and incident acoustic pressure.

MATERIALS AND METHODS

Phantom design

The novel phantom designed to hold the contrast agent was manufactured in three sections and formed within a plastic casing (Fig. 1). The upper and lower sections, of 4-cm and 3-cm depth, respectively, were made from tissue-mimicking material (Teirlinck et al. 1997, 1998). In this latter reference, the size of the aluminium oxide scatterers was incorrectly stated. The actual composition should include 3 μm and 0.3 μm Al_2O_3 particles, rather than the 3-mm and 0.3-mm quoted values) and the centre section from an anechoic

material (3-cm depth). The dimension of the lower section (3 cm) was chosen to represent a typical distance between a transducer probe placed on the surface of the skin and the heart muscle from either a parasternal long-axis view or an apical view. The anechoic medium was manufactured by adapting the tissue-mimicking material, whereby the silicon carbide and aluminium oxide particles that form the major scatterers of the tissue-mimicking material were omitted from the recipe. Within the anechoic material, and in the same plane, two identical 20 mm \times 20 mm \times 1 mm slots were made. The 1-mm width of the slot was chosen so as to be less than the sector slice thickness, to ensure that all the contrast agent microbubbles were insonated in every ultrasonic frame.

A channel was manufactured from the base of one of these slots to the external casing of the phantom to facilitate injection, removal and flushing of the contrast into and out of the phantom. In the other slot, a 20 mm \times 20 mm \times 1 mm slice of tissue-mimicking material was inserted. Measurements of ultrasonic backscatter from this slice of tissue-mimicking material served as our reference for backscatter measurements made from contrast microbubbles.

A rectangular hole was cut in the external casing to allow the transducer probe access to scan the phantom. After completion, the phantom was mounted on a supporting rig. The transducer probe was positioned below the tissue-mimicking phantom and coupled to the lower surface of the phantom using US gel.

Table 1. Parameters describing physical features of three ultrasonic contrast agents used in this study

Agent	Manufacturer	Type of agent	Capsule	Gas	Bubble diameter	Concentration	Clinical recommended dose
Sonazoid®	Nycomed	information not available	surfactant	fluorocarbon	median 3.2 μm	1% gas volume/volume suspension (measured)	3 $\mu\text{L/kg}$
Definity® (DMP-115)	ImaRx/DuPont	encapsulated bubble	lipid	perfluoropropane	mean 2.5 μm	10×10^8 bubbles/mL	3–5 $\mu\text{L/kg}$
Optison®	Mallinckrodt	encapsulated microsphere	albumin	octafluoropropane	mean 3.7 μm	$5\text{--}8 \times 10^8$ $\mu\text{bubbles/mL}$	1 mL @ fundamental; 0.5 mL @ second harmonics

Ultrasound scanner

The phantom was insonated using an Acuson XP-10, V4C phased-array probe operating at a central frequency of 4 MHz. The probe was coupled to the phantom, so that the complete slot into which contrast was to be injected could be visualised in the scan plane. The depth of the field of view was set at 12 cm and the focus was set at 7 cm. The TGC settings were set at midvalues and the gain was maintained at 0 dB during all experiments. The Acuson XP-10 had four output power settings (0 dB, –3 dB, –6 dB and –9 dB). The scanner was set initially at maximum output power (0 dB).

The Acuson XP-10 had been modified to allow access to the unprocessed analogue US signal data. Using the same digitising equipment and memory storage detailed in Moran *et al.* (1998), the analogue signal was digitised to 12 bits at a rate of 20 M samples/s. Due to storage limitations, a maximum of 38 frames of data were collected during each data acquisition. However, using the ECG-triggering mode and additional hardware, it was possible to control collection of these 38 frames in a predetermined sequence. Dependent on the rate of decay of the backscatter signal, the ultrasonic data could be acquired every frame, every alternate frame, every fourth, eighth, sixteenth or thirty-second frame of insonation.

Contrast agents

Three IV fluorocarbon-filled contrast agents were studied. These were Sonazoid® (Nycomed, Oslo, Norway; currently undergoing phase III clinical trials), Optison® (Mallinckrodt, Hennep, Germany; a commercially available contrast agent) and Definity® (DuPont, North Billenica, MA; an agent currently undergoing clinical trials in the USA). The properties of these agents are detailed in Table 1.

Assuming that the Definity® and Optison® microbubbles are spherical in shape and that, for each agent, all the microbubbles have diameters equal to the mean diameter, the gas volume/suspension volume ratios are

equal to 8.2×10^{-3} and 17.2×10^{-3} , respectively. From the manufacturer's details, Sonazoid® has a measured 10×10^{-3} gas volume /suspension volume ratio.

The dilution of the agents was chosen on the basis of being able just to visualise both the proximal and distal edges of the contrast-filled slot during the first frame of insonation, when insonated at maximum power output. On this basis, the Definity® agent was diluted to 1:1000, resulting in a calculated gas volume of 8.18 nL/mL of solution. Optison® was diluted to 1:2000, resulting in a calculated gas volume of 8.6 nL/mL of solution. The dilutant used for Optison® and Definity® was sterile water. The Sonazoid® agent, as per manufacturer's recommendations, was diluted with a 5% dextrose solution to a 1:2500 concentration. This resulted in a calculated gas volume of 4 nL/mL of solution.

Acquisition of data

Two mL of the diluted contrast solution were drawn up in a syringe that was then mounted on the external casing of the phantom *via* a cannula (Fig. 1). The scanner was placed in Freeze mode (*i.e.*, no acoustic output) and the contrast was slowly injected into the phantom *via* the channel detailed above. After the injection was complete, the scanner was released from Freeze mode and the contrast agent was insonated. Over the period of insonation, a total of 38 frames of data were collected. After the data were digitised and stored, the slot was repeatedly flushed with sterile water, prior to the next injection of contrast. To assess the reproducibility of the results, each insonation at a particular output setting and for each contrast agent was repeated 3 times.

After the measurements of contrast agent backscatter were complete for each agent and for each output power, the transducer probe mounting was adjusted so that the reference tissue-mimicking slot was insonated. Measurements were made at the four output settings of the scanner. These data were also digitised and stored on the workstation.

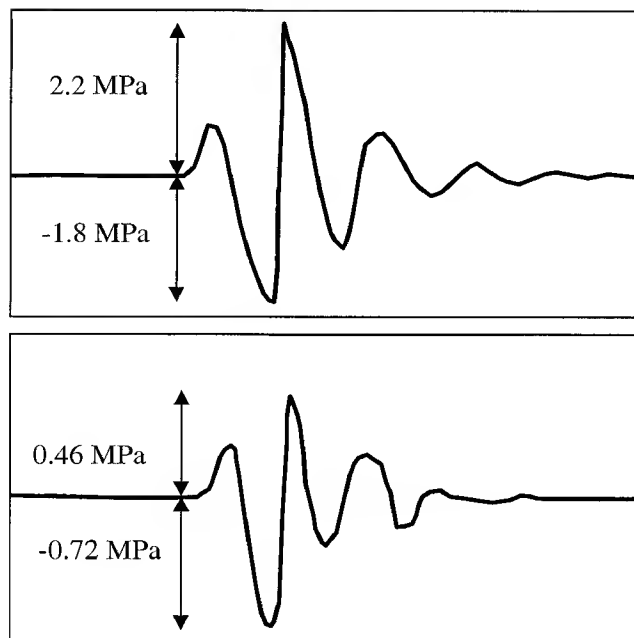


Fig. 2. Acoustic pulse-shapes measured using 0.2-mm needle hydrophone at maximum power output (0 dB). Upper pulse measured after US pulse had travelled 5 cm in water. Lower pulse obtained within the water-filled phantom-slot at a distance of 5 cm from probe.

Acoustic pressure measurements

After collection of the data from the contrast agents, the slot was injected with water. The transducer probe was mounted as previously described and the phantom was insonated. In this instance, however, to facilitate measurement of the acoustic pressure field within the phantom, the upper section of the phantom was removed. This enabled a PVDF needle hydrophone (0.2 mm diameter active area, model HPM02/1; Precision Acoustics Ltd., Dorchester, UK) to be introduced into the slot using a micromanipulator. Under US visualisation, the tip of the needle hydrophone was placed in the centre of the slot, at a distance of 5 cm from the transducer probe. Measurements were taken of the amplitude of the acoustic pressure pulse at the four output powers of the scanner. The needle hydrophone was then calibrated by mounting it in a water bath at a distance of 5 cm from the transducer probe and calibrating these results (Fig. 2) against those obtained at the same distance using a 0.5-mm PVDF membrane hydrophone that had been calibrated at the National Physical Laboratory (Teddington, UK).

To assess the decrease in pressure across the 2-mm slot, the distance between the needle hydrophone and transducer probe was fixed at 50 mm, and the position of peak negative pressure was established. Using the micromanipulator, the hydrophone was then moved 1 mm

off axis. Peak negative pressure decreased by -2.2 dB at a distance of 1 mm off-axis at the centre of the slot.

Analysis

After the data from the contrast slot were digitised and stored, they were analysed using a program developed in-house (Moran et al. 1998) and reviewed briefly here. The data were scan-converted and log-compressed to yield images almost visually identical to those displayed on the scanner. This allowed accurate positioning of a 2-cm square region of interest (ROI) over the contrast-filled slot. The mean backscatter from the slot was then calculated from the original unprocessed US data. All the values were then normalised by reference to the mean backscatter value from an identical ROI placed within the tissue-mimicking slot. Converting into the decibel notation yielded the integrated backscatter, eqn (1), and the mean of the three integrated backscatter values from the three experimental data sets gave the mean integrated backscatter values.

$$\text{Integrated backscatter} = 10 \log_{10} \left(\frac{\int_{t-\Delta t}^{t+\Delta t} |V(t)|^2 dt}{\int_{t-\Delta t}^{t+\Delta t} |R(t)|^2 dt} \right), \quad (1)$$

where $V(t)$ is the instantaneous amplitude of the unprocessed signal (at time t) from the contrast-enhanced ROI, $R(t)$ is the instantaneous amplitude of the unprocessed signal from the tissue-mimicking material ROI and t is the centre of the time-gate centred on the slot. The data were digitised at a rate of 20 M samples/s giving a calculated dt size of 50 ns. Digitisation at these rates ensured unaliased capture of frequencies up to 10 MHz. Assuming a speed of sound of 1540 m/s, the width of the capture gate, t , was equal to 13.0 μ s, resulting in 258 data points along each scan line lying within the time-gate. Assuming a 90° sector scan, composed of 128 scan lines at a depth of 5 cm, a calculated 32 lines passed through a 2-cm wide box. Consequently, the mean integrated backscatter calculated over the ROI was from a population of 8256 backscatter data points.

RESULTS

The data displayed in Figs. 3, 4 and 5 correspond to the mean integrated backscatter from three sets of data. The error bars displayed on the graphs correspond to the standard deviation of the measurements. The four series in Figs. 3, 4 and 5 correspond to the four output power levels displayed on the Acuson XP-10. The correspond-

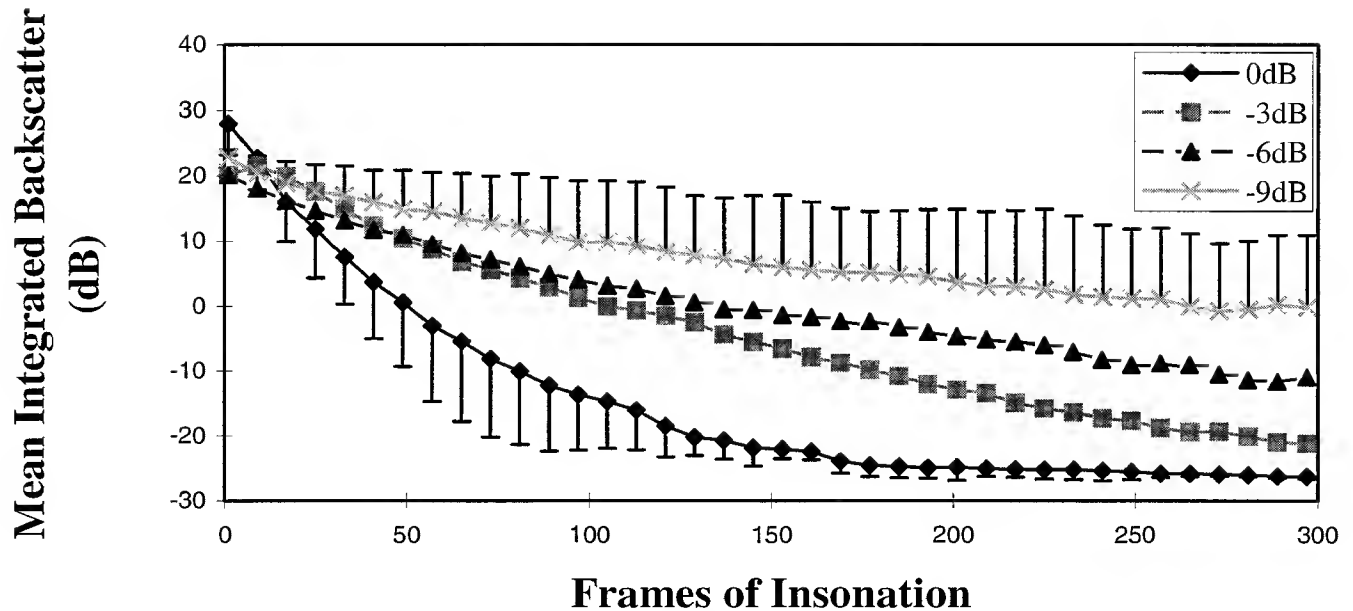


Fig. 3. Mean integrated backscatter vs. number of frames of insonation for Definity® at four acoustic output powers. 300 frames corresponds to approximately 8.9 s of insonation.

ing measurement of peak negative pressure using the 0.2-mm needle hydrophone at the four output power levels is displayed in Table 2.

For Definity® (Fig. 3) and Sonazoid® (Fig. 5), the unprocessed US information was acquired from every eighth frame of insonation. For Optison® (Fig. 4), be-

cause of the rapid decrease in mean integrated backscatter as a function of the number of frames of insonation, the unprocessed US data were acquired from every frame of insonation. At the depth and focus chosen, the frame-rate of the scanner was 34 Hz. Because 38 unprocessed frames of data were acquired in total, the x-axis of the

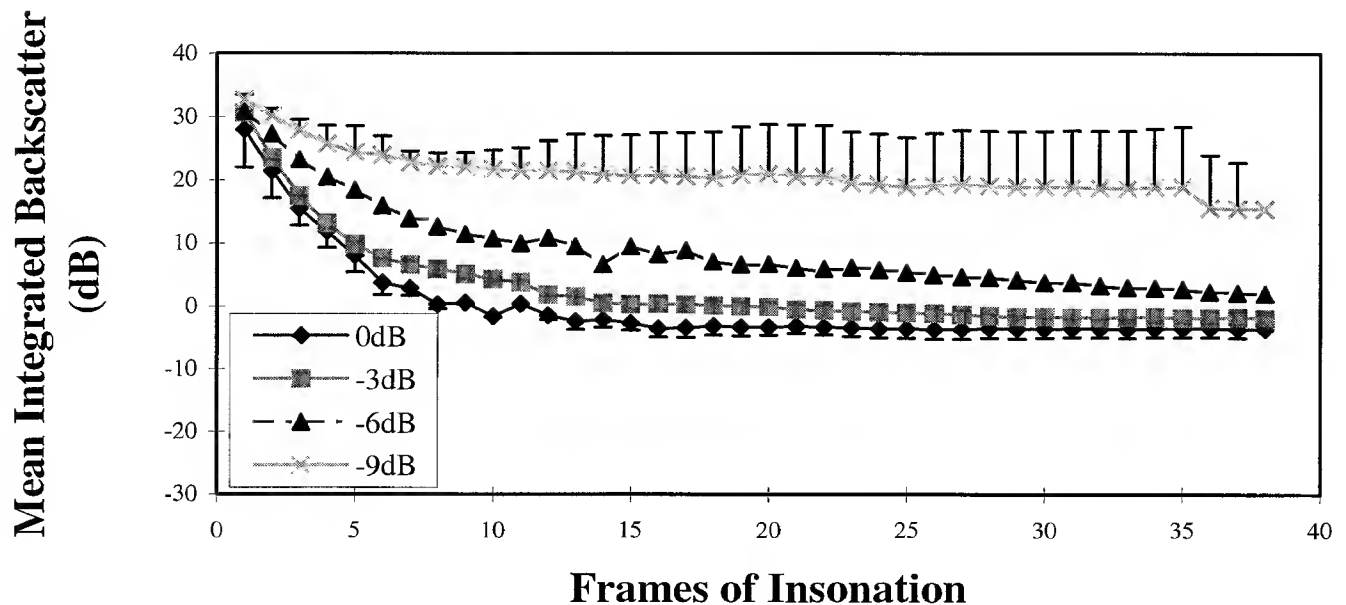


Fig. 4. Mean integrated backscatter vs. number of frames of insonation for Optison® at four acoustic output powers. 38 frames corresponds to approximately 1.1 s of insonation.

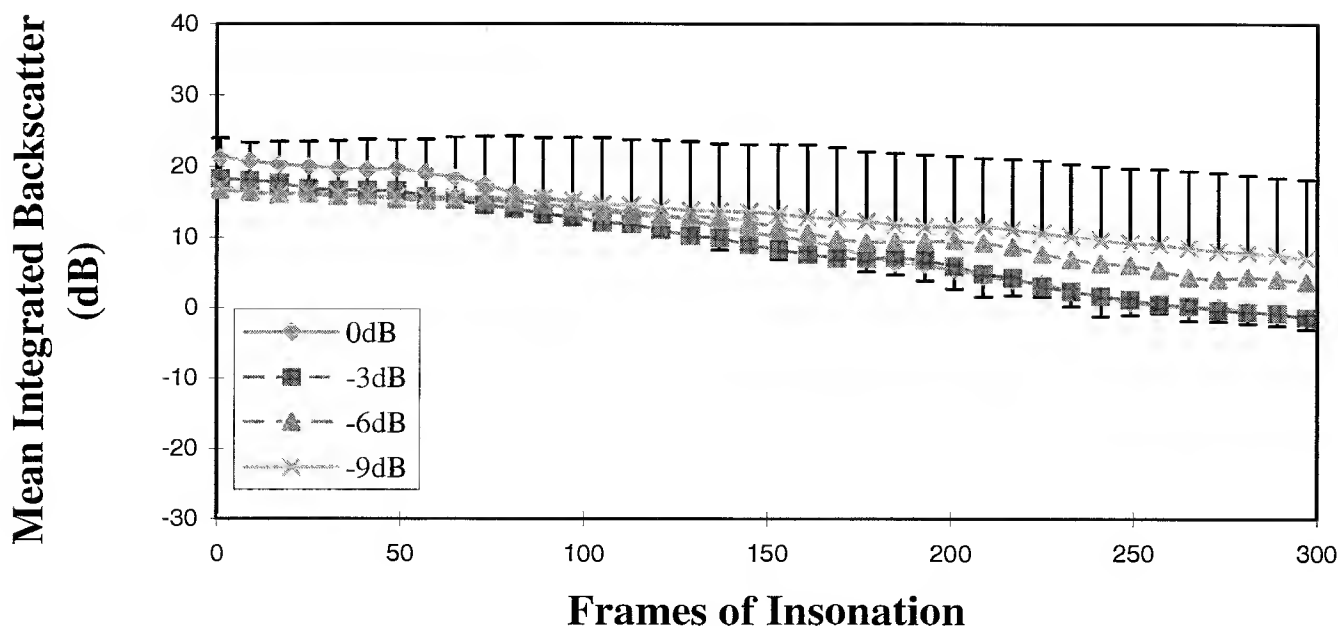


Fig. 5. Mean integrated backscatter vs. number of frames of insonation for Sonazoid® at four acoustic output powers. 300 frames corresponds to approximately 8.9 s of insonation.

graphs displayed in Figs. 3 and 5 correspond to a period of insonation of approximately 8.9 s and, in Fig. 4, to a period of insonation of approximately 1.1 s.

The data collected from Definity® are displayed in Fig. 3. Note that the mean integrated backscatter from the first frame of insonation at all power outputs is at least 20 dB greater than that displayed by the tissue-mimicking material. In addition, as is also evident from Table 3, at higher acoustic power outputs there is a more rapid decrease in mean integrated backscatter than at lower power outputs. Indeed, at the maximum output power level (0 dB), the mean integrated backscatter values decrease rapidly and reach a minimum value of -25 dB after approximately 160 frames of insonation (\approx 4.7 s). The relative longevity of this minimum value

would suggest that no further change in mean integrated backscatter is likely as a result of further insonation. For lower power outputs, although there is a decrease in mean integrated backscatter, no such plateau is observed.

Figure 4 illustrates the mean integrated backscatter vs. number of frames of insonation for Optison® at the four output powers of the scanner. As is evident from the graph, the mean integrated backscatter values from the agent were at least 25 dB higher than the mean integrated

Table 2. Peak negative pressures at 50-mm distance between transducer probe and hydrophone measured using 0.2-mm PVDF needle hydrophone as a function of nominal power output display on Acuson XP-10

Nominal power output displayed on Acuson scanner (dB)	Peak negative pressure (MPa)	Actual power output (dB)
0	-0.72	0
-3	-0.49	-3.3
-6	-0.34	-6.5
-9	-0.23	-9.9

The third column displays the actual power outputs calculated using the peak negative pressures in the second column.

Table 3. Least squares line fits to the data displayed in Figs. 3, 4 and 5

(dB)	Gradient (dB/frame) $\times 10^{-3}$	Intercept (dB)	Correlation coefficient
Definity®			
0	-326 (160 frames)	19.9	0.93
-3	-140	17.6	0.97
-6	-98	15.4	0.96
-9	-72	18.5	0.95
Sonazoid®			
0	-84	22.7	0.99
-3	-71	19.3	0.99
-6	-47	18.0	0.96
-9	-33	17.6	0.96
Optison®			
0	-3400 (10 frames)	27.5	0.92
-3	-3000 (10 frames)	28.5	0.87
-6	-2400 (10 frames)	31.4	0.96
-9	-1300 (10 frames)	32.3	0.90

For Optison®, the line fits were fitted only to the data acquired from the first 10 frames of insonation and, for Definity® at 0 dB, for the first 160 frames.

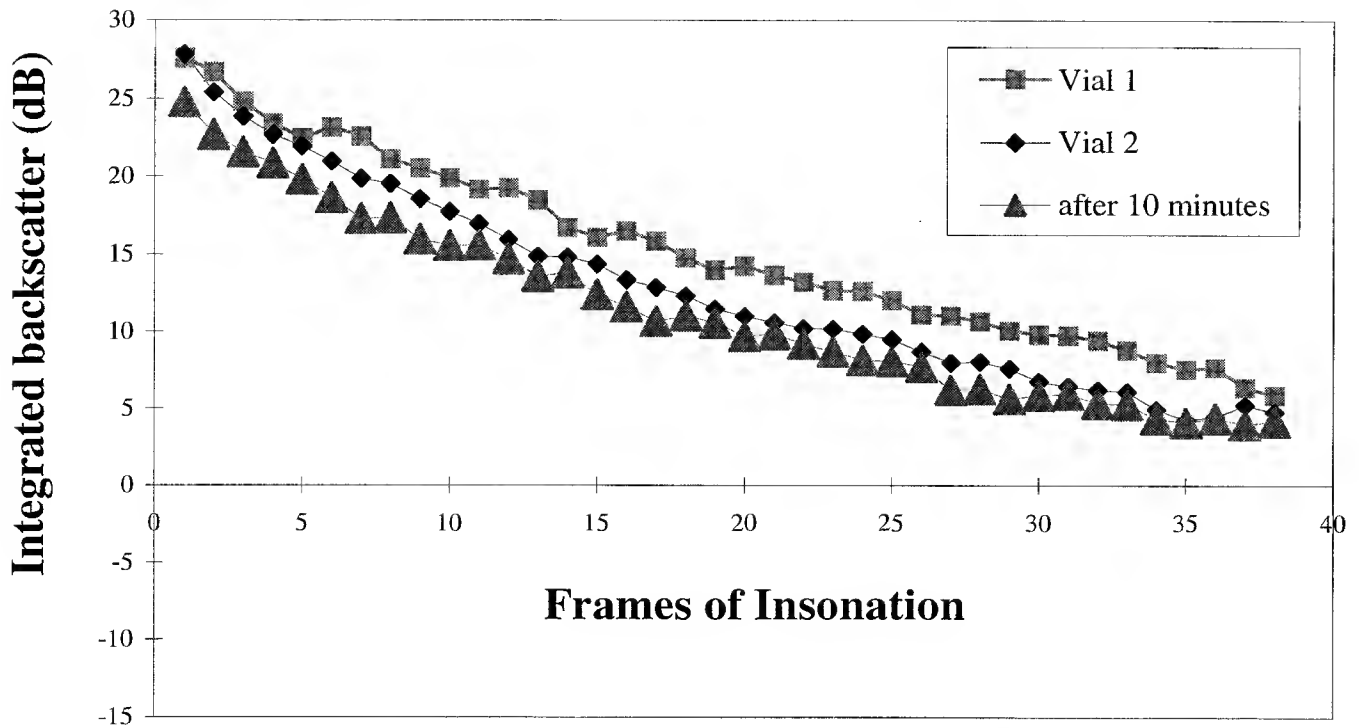


Fig. 6. Integrated backscatter vs. number of frames of insonation from three samples of Definity®: two samples diluted from independent vials; the third sample diluted and left for 10 min before insonation.

backscatter from the tissue-mimicking material. In a similar manner to Definity®, Optison® demonstrated a marked sensitivity to higher acoustic output powers (see Table 3). For this agent, the plateau in mean integrated backscatter is achieved after approximately 15 frames of insonation (≈ 0.44 s) and is evident not only at the 0-dB (maximum) output power level but also at the -3-dB reduced output power level.

Figure 5 illustrates the mean integrated backscatter vs. number of frames of insonation for Sonazoid®. At the concentrations used in the experiment, the mean integrated backscatter from the first frames of insonation is at least 17 dB greater than the tissue-mimicking material. In addition, Sonazoid® demonstrates a reduced rate of decrease in mean integrated backscatter in comparison to Definity® at all power outputs (Table 3).

SOURCES OF ERROR

As described previously, each experiment was repeated 3 times. The data displayed in Figs. 3, 4 and 5 are the means of these data. The standard deviation of these measurements for the 0-dB and -9-dB data sets are displayed as error bars (in one direction for clarity) on the figures. For all three agents, standard deviations were highest for the lowest power level.

To determine the variability between different vials,

two fresh samples from two different vials were independently diluted and then injected into the phantom and insonated within 30 s after dilution. Insonation was set at 0-dB power output level. These data are named vial 1 and vial 2 in Figs. 6, 7 and 8.

To determine if the effects observed were due to some other external parameter (e.g., dilutant, time after preparation etc.), an additional contrast sample, from vial 2, was diluted and left for 10 min. After a period of 10 min had elapsed, the agent was gently agitated to ensure a homogeneous solution, and a sample was drawn up in the syringe and injected into the phantom. In the main experimental protocol, the agent was diluted no more than 10 min prior to injection into the phantom. Insonation took place at 0 dB. The integrated backscatter values for these curves are also shown in Figs. 6, 7 and 8 and labelled "after 10 minutes."

For all three agents, the magnitude of the integrated backscatter values from the samples taken from two independent vials and insonated within 30 s, lay within 1 standard deviation of the calculated means illustrated in Figs. 3, 4 and 5. A comparison of the integrated backscatter values obtained from the samples showed that those obtained directly after dilution were significantly larger than those obtained 10 min after dilution. However, the gradients calculated from all three samples from

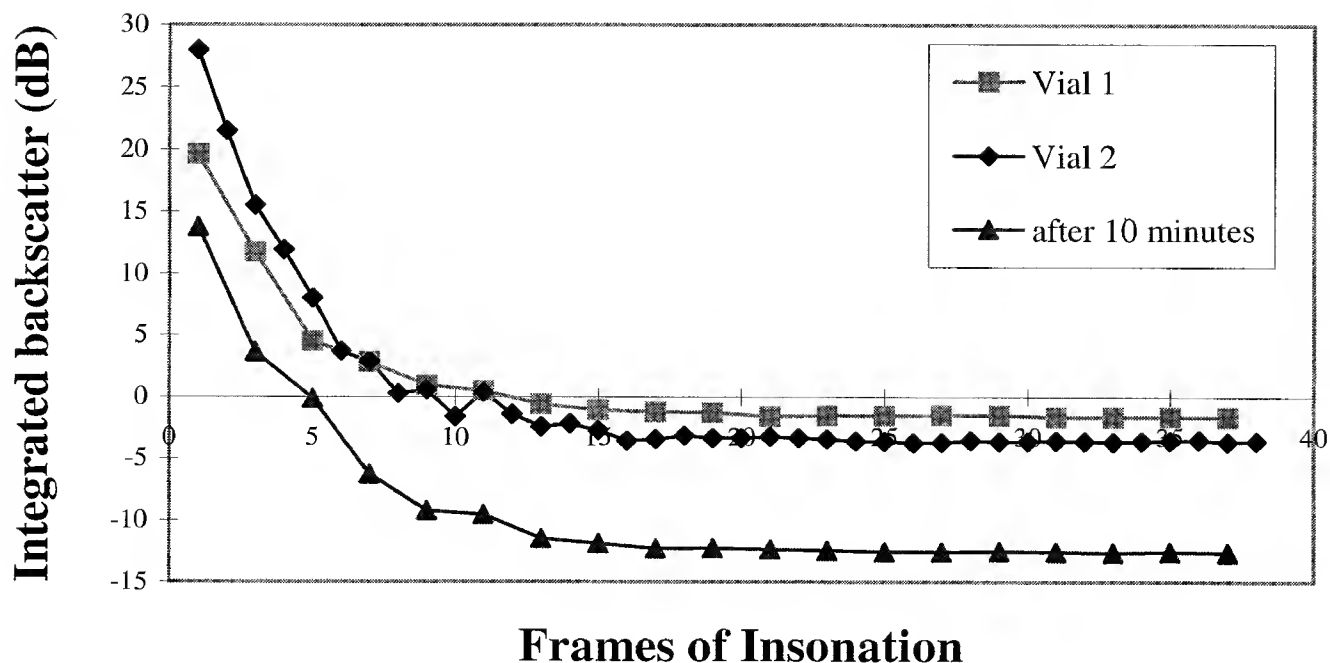


Fig. 7. Integrated backscatter vs. number of frames of insonation from three samples of Optison®: two samples diluted from independent vials; the third sample diluted and left for 10 min before insonation.

each agent were not significantly different ($p < 0.05$) (see Table 4). Note that, in this reproducibility experiment, backscatter data were collected over only 38 frames of insonation. In particular, for Definity®, a comparison of the intercepts and gradients of the line-fits calculated over these 38 frames of insonation (Table 4)

and those calculated over 160 frames of insonation (Table 3) highlighted significant differences. However, by applying a least squares fit to the mean integrated backscatter data from Definity®, only over the initial 38 of the 160 frames of insonation were intercepts and gradients comparable to those collected in this reproducibility ex-

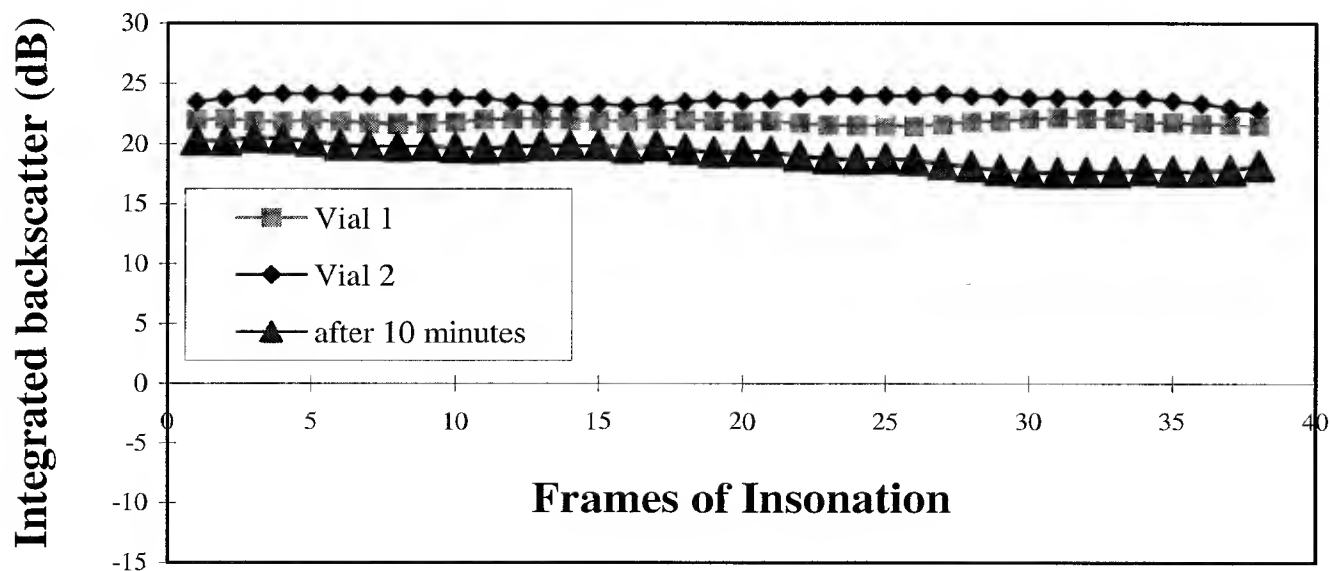


Fig. 8. Integrated backscatter vs. number of frames of insonation from three samples of Sonazoid®: two samples diluted from independent vials; the third sample diluted and left for 10 min before insonation.

Table 4. Least squares line fits to the data displayed in Figs. 6 and 7 for Definity® and Optison®, respectively

	Gradient (dB/frame) $\times 10^{-3}$	Intercept (dB)	Correlation coefficient
Definity®			
Vial 1	-530 (38 frames)	25.6	0.97
Vial 2	-570 (38 frames)	24.1	0.95
10 min	-520 (38 frames)	21.5	0.95
Fig. 3 data	-326 (initial 160 frames)	19.9	0.93
Fig. 3 data	-574 (initial 38 frames)	27.3	0.93
Optison®			
Vial 1	-3400 (10 frames)	27.5	0.92
Vial 2	-2700 (10 frames)	22.3	0.85
10 min	-2590 (10 frames)	19.9	0.86

The line-fits for Definity® were fitted to the data from the 38 frames, those for Optison® were fitted to the data required from the first 10 frames of insonation. In addition, the results from the least-squares line fit for Definity® data acquired at 0 dB over the initial 160 frames and over the initial 38 frames are also displayed.

periment (Table 4). For Sonazoid®, no significant decrease in integrated backscatter was observed over the initial 38 frames of insonation.

DISCUSSION

Dayton et al. (1999) have elegantly shown, both optically and acoustically, the effect of shell and gas composition on the acoustic backscatter properties of single contrast microbubbles. In their paper, both albumin-encapsulated (Optison®) and lipid-encapsulated microbubbles (not Definity®) were tethered to a polystyrene plate. Acoustic pressures were measured and were similar in magnitude to those measured at the lowest power setting (-9 dB) described in this paper. They were able to observe that the most common mode of destruction at these lower acoustic pressures was a gradual reduction of the bubble size as gas slowly diffused out. As acoustic pressure increased, they observed an increasing number of albumin-encapsulated agents developing defects in their shells, allowing the gas to escape. The mean survival time of these free gas bubbles was 280 ms (which corresponds to 9 frames of insonation at a frame rate of 34 Hz, as used in the studies presented in this paper). At higher acoustic pressures, they also observed that some lipid-encapsulated and albumin-encapsulated microbubbles disappeared after a single pulse of insonation, suggesting that, at higher pressures, the large bubble may break into several smaller bubbles that diffuse more rapidly into solution. It is this latter phenomenon that we assume is exploited in the determination of myocardial blood velocity.

In addition, Klibanov et al. (1998), using single microbubble imaging techniques, have likewise shown that higher concentrations of microbubbles, lower US

transmit power settings and triggered imaging each can reduce the rate of destruction of microspheres resulting from medical US insonation.

In our study, we have looked at the effects of acoustic pressure on large concentrations of microbubbles (on the order of 10^5 microbubbles/mL). Tethering the microbubbles may cause them to behave differently from microbubbles suspended in an isotropic medium. To overcome this problem, we have designed and manufactured a phantom that permits the microbubbles to move between frames of insonation but not outside the US beam. No new contrast is injected between frames, so the effects observed are as a result of the interaction of the US beam and the contrast microbubbles.

Optison®

Optison® demonstrates a marked sensitivity to the US pressure, with the mean integrated backscatter falling more rapidly at higher pressures than at lower pressures. For Optison® at low acoustic pressures (-9 dB), after an initial decrease in mean integrated backscatter, a plateau appears to be reached at approximately 20 dB, from which, over the remaining 38 frames, there was little variation in mean integrated backscatter. This would seem to suggest that some of the microbubbles are more robust than others and can survive unaltered at low acoustic pressures. Moreover, even at maximum acoustic pressure, some of these microbubbles may still survive because the plateau of mean integrated backscatter for Optison® microbubbles, when insonated at maximum pressure, lies at a value of approximately 0 dB (*i.e.*, equivalent to the mean integrated backscatter from the tissue-mimicking material). This is approximately 26 dB greater than the corresponding plateau observed from Definity® after similar insonation conditions. It must be noted that Optison® was studied over a much shorter time, but our initial studies suggest that some Optison® microbubbles are robust in nature and are not destroyed even at high acoustic outputs. An alternative explanation is put forward by Frinking et al. (1999). The results from their study, using air-filled albumin-encapsulated bubbles, suggest that the encapsulated air is replaced by the surrounding liquid. As a result, because liquid-filled microbubbles are less compressible than gas-filled microbubbles, they become less effective scatterers.

Definity®

After dilution, both Optison® and Definity® solutions have approximately the same calculated gas volume. The plateau of mean integrated backscatter from Definity® lies at -26 dB for a scanner power output of 0 dB. This is achieved after 160 frames of insonation, suggesting that all the Definity® microbubbles have been destroyed. From the work of Dayton et al. (1999), it

would appear that the most likely destruction process for Definity® is that the US beam produces a defect in the microbubble shell and a gas bubble is formed that rapidly breaks into smaller, more easily diffusible, bubbles. At lower acoustic output pressures, the mean integrated backscatter from Definity® continues to decrease linearly with increasing number of frames of insonation, but not as rapidly as higher acoustic pressures. This would suggest that a somewhat different destruction process is ongoing, perhaps a more gentle deflation of the microbubble.

It is likely that, with both Optison® and Definity®, a combination of different destruction phenomena take place within the slot. Although we have measured the acoustic pressure in the centre of the slot, contrast proximal to the transducer probe will cause attenuation and, thus, reduce the acoustic pressure on contrast microbubbles more distal from the transducer probe. This is likely to affect the destruction processes that take place within the contrast slot.

Sonazoid®

The composition of the shell of the Sonazoid® microbubbles was not known. This agent showed less sensitivity to different acoustic pressures than either Definity® or Optison®. The gas volume/volume solution was approximately 50% of that calculated for the other agents, and the Sonazoid® microbubbles were diluted in glucose rather than in sterile water, as per the manufacturer's recommendations. For Optison® and Definity®, the intercepts with the mean integrated backscatter axis were 26.9 dB and 27.9 dB, respectively. For Sonazoid®, the intercept was only 21.2 dB. The decrease in backscatter with number of frames of insonation for Sonazoid® was much less pronounced than for Definity® or Optison®; thus, providing a much longer period of enhancement at higher acoustic pressures. Without knowledge of the specific constituents of the shell, it is difficult to hypothesise further on the possible modes of destruction of Sonazoid® microbubbles.

For the three agents in this study, one frame of insonation was not sufficient to destroy all the contrast agent microbubbles within the slot, even at dilutions of 1:1000 and at maximum power output. Two methods are currently proposed for the assessment of myocardial blood velocity. First, contrast microbubbles are either infused or bolus-injected and the triggered imaging rate is varied, so that an accurate map of the intervals between microbubble destruction and time for contrast re-enhancement may be made (Porter and Xie 1995). Alternatively, the contrast agent is infused and, by initially destroying the agent and subsequently maintaining a constant triggered image frame and varying the flow rate, a map of mean microbubble velocities may be built

up (Wei et al. 1998). Both techniques assume that, at high acoustic outputs, one US pulse effectively destroys all the contrast agent microbubbles. We have shown, in this study, that, even at maximum power output of a routinely used clinical scanner insonating through 3 cm of tissue-mimicking material, none of the agents exhibited the sensitivity to acoustic pressure necessary for the assessment of myocardial blood velocity using the methods described above.

Consequently, for those agents that are robust and require a larger acoustic pressure for shell defects to be formed or for larger patients who have more substantial attenuating overlying layers of tissue, it may not be possible to use these techniques for mapping myocardial blood velocities.

CONCLUSIONS

In this study, we have investigated the acoustic sensitivity of three contrast agents as a function of acoustic pressure. To do this, we have developed and manufactured a novel and versatile phantom that ensures that the microbubbles remain within the US beam with minimal mechanical interference.

All three agents demonstrated a measurable sensitivity to acoustic pressure. Sonazoid® demonstrated least sensitivity to the acoustic pressure, suggesting that the microbubbles have a very robust shell. Optison® was most sensitive to acoustic pressure over the initial 10 frames of insonation, its sensitivity then rapidly disappearing, suggesting that perhaps there are some robust microbubbles within the Optison® composition. Definity® demonstrated a very distinct sensitivity to acoustic pressure, suggesting a uniformity in the composition of the Definity® microbubbles.

Acknowledgements—Dr. Carmel Moran and Tom Anderson are currently funded under a British Heart Foundation Project Grant.

REFERENCES

- Chang PH, Shung KK, Wu SJ, Levene HB. Second harmonic imaging and harmonic Doppler measurements with Albunex. *IEEE Trans Ultrason Ferroelec Freq Control* 1995;42:1020–1027.
- Church CC. The effect of an elastic solid surface layer on the radial pulsations of gas bubbles. *J Acoust Soc Am* 1995;97:1510–1521.
- Dayton PA, Morgan KE, Klibanov AL, Brandenburger GH, Ferrara KW. Optical and acoustical observations of the effects of ultrasound on contrast agents. *IEEE Trans Ultrason Ferroelec Freq Control* 1999;46:220–232.
- DeMaria AN, Cotter B. Myocardial contrast echocardiography: too much, too soon? *J Am Coll Cardiol* 1998;32:1270–1271.
- Frinking PJA, de Jong N, Cespedes EI. Scattering properties of encapsulated gas bubbles at high ultrasound pressures. *J Acoust Soc Am* 1999;105:1989–1996.
- Klibanov AL, Ferrara KW, Hughes MS, Wible JH, Wojkyla JK, Dayton PA, Morgan KE, Brandenburger GH. Direct video-microscopic observation of the dynamic effects of medical ultrasound on ultrasound contrast microspheres. *Invest Radiol* 1998;33:863–870.
- Linka AZ, Sklenar J, Wei K, Jayaweera AR, Skyba DM, Kaul S.

- Assessment of transmural distribution of myocardial perfusion with contrast echocardiography. *Circulation* 1998;98:1912–1920.
- Marwick TH, Brunken R, Meland N, Brochet E, Baer FM, Binder T, Flachskampf F, Kamp O, Nienaber C, Nihoyannopoulos P, Pierard L, Vanoverschelde J-L, Wouw P, Lindvall K. Accuracy and feasibility of contrast echocardiography for detection of perfusion defects in routine practice. Comparison with wall motion and technetium-99m sestamibi single-photon emission computed tomography. *J Am Coll Cardiol* 1998;32:1260–1269.
- Moran CM, Anderson T, Sboros V, Sutherland GR, Wright R, McDicken WN. Quantification of the enhanced backscatter phenomenon from an intravenous and an intra-arterial contrast agent. *Ultrasound Med Biol* 1998;24:871–880.
- Pelberg RA, Wei K, Kamiyama N, Sklenar J, Bin J, Kaul S. Potential advantage of flash echocardiography for digital subtraction of B-mode images acquired during myocardial contrast echocardiography. *J Am Soc Echocardiogr* 1999;12:85–93.
- Porter TR, Xie F. Transient myocardial contrast after initial exposure to diagnostic ultrasound pressures with minute doses of intravenously injected microbubbles. *Circulation* 1995;92:2391–2395.
- Porter TR, Shouping L, Kricsfeld D, Armbruster RW. Detection of myocardial perfusion in multiple echocardiographic windows with one intravenous injection of microbubbles using transient response second harmonic imaging. *J Am Coll Cardiol* 1997;29:791–799.
- Schrope B, Newhouse VL, Uhlendorf V. Simulated capillary blood flow measurement using a non-linear ultrasonic contrast agent. *Ultrasonic Imaging* 1992;14:134–158.
- Simpson DH, Chin DT, Burns PN. Pulse inversion Doppler: a new method for detecting non-linear echoes from microbubble contrast agents. *IEEE Trans Ultrason Ferroelec Freq Control* 1999;40:372–382.
- Strauss AL, Beller KD. Persistent opacification of the left ventricle and myocardium with a new echo contrast agent. *Ultrasound Med Biol* 1999;25:763–769.
- Teirlinck CJPM, Bezemer RA, Kollmann C, Lubbers J, Hoskins PR, Ramnarine KV, Fish P, Fredfeldt K-E, Schaarschmidt UG. Development of an example flow test object and comparison of five of these test objects constructed in various laboratories. *Ultrasonics* 1998;36:653–660.
- Tierlinck CJPM, Fish P, Hoskins PR, et al. Validation of a flow Doppler test object for diagnostic ultrasound scanners. EC TNO Report contract MAT-CT 940091. Leiden: TNO Prevention and Health, 1997.
- Wei K, Jayaweera AR, Firoozan S, Linka A, Skyba DM, Kaul S. Quantification of myocardial blood flow with ultrasound-induced destruction of microbubbles administered as a constant venous infusion. *Circulation* 1998;97:473–480.
- Wei K, Skyba DM, Firsckhe C, Jayaweera AR, Lindner JR, Kaul S. Interactions between microbubbles and ultrasound: in vitro and in vivo observations. *J Am Coll Cardiol* 1997;29:1081–1088.